ARTICLE

Nucleation of Kinetic Ising Model Under Oscillating Field

Kun Li[a], Hui-jun Jiang[a], Han-shuang Chen[c], Zhong-huai Hou[a,b]*

a. Department of Chemical Physics, University of Science and Technology of China, Hefei 230026, China
b. Hefei National Laboratory for Physical Sciences at the Microscale, University of Science and Technology of China, Hefei 230026, China
c. School of Physics and Material Science, Anhui University, Hefei 230039, China

(Dated: Received on April 5, 2012; Accepted on May 2, 2012)

We have studied the nucleation process of a two-dimensional kinetic Ising model subject to a bias oscillating external field, focusing on how the nucleation time depends on the oscillation frequency. It is found that the nucleation time shows a clear-cut minimum with the variation of oscillation frequency, wherein the average size of the critical nuclei is the smallest, indicating that an oscillating external field with an optimal frequency can be much more favorable to the nucleation process than a constant field. We have also investigated the effect of the initial phase of the external field, which helps to illustrate the occurrence of such an interesting finding.

Key words: Kinetic Ising model, Nucleation, Oscillating field

I. INTRODUCTION

Nucleation is a fluctuation-driven process that initiates the decay of a metastable state into a more stable one [1]. Many phenomena in nature are associated with nucleation, such as crystallization [2], glass formation [3, 4], and protein folding [5]. The Ising model is a simple but powerful model which has been widely used to study the nucleation process. For instance, the nucleation pathway of the Ising model in a three-dimensional lattice has been studied by the transition path sampling approach in which analysis of the transition state ensemble (TSE) indicate that the critical nuclei are rough and anisotropic [6]. Ising model in the geometry of a long stripe exhibits a rather different "phase behavior" from bulk phase transition, and it was demonstrated that this system exhibits properties of the 2D Ising bulk system as well as properties of the 1D-Ising system [7]. The existence of a pore may change the nucleation mechanics, leading to two-stage nucleation and the overall nucleation rate can arrive at a maximum level in intermediate pore size [8]. Ising model has also been used to test the applicability of the classical nucleation theory by Shneidman *et al.* [9], and so on.

Despite great progress, the physics of nucleation has been made in "quasi equilibrium" systems. Nucleation also takes place in systems out of equilibrium. In recent decades, nucleation in driven systems where external forces break the detailed balance has gained more and more attention, including nucleation of glasses [4], semicrystalline polymers [10], and microcellular foaming process under shear. Simulations and experiments reveal that shear has a significant impact on nucleation and nonequilibrium phase transitions [10, 11]. Blaak *et al.* found shear can suppress nucleation and lead to a larger critical nucleus [12]. Mazzanti *et al.* reported that crystalline orientation and phase transition acceleration induced by shear are demonstrated to occur in different edible fats using synchrotron X-ray diffraction [13]. In the 2D (two-dimension) Ising system, shear can enhance nucleation rate and at intermediate shear rate the nucleate-rate peaks [14].

Oscillating field usually acts as an important type of driven force in nonequilibrium systems. Ising models subject to an oscillating field have been used to study the so-called dynamic phase transition (DPT). After first observed by Tomé [15], DPT had been extensively studied by mean field analysis [15, 16], Monte Carlo (MC) simulations [17−19], and other analytical methods [20, 21]. It is found that the critical exponent of the DPT is consistent with the equilibrium Ising value, which is universal with respect to the choice of the stochastic dynamics [22]. Nevertheless, nucleation process of the Ising system under oscillating field has not been studied yet.

In the present work, we have investigated the nucleation of a 2D kinetic Ising model subject to an oscillating external field using MC simulations. We have mainly focused on how the nucleation time τ_n, defined as the ensemble averaged escape time from the metastable state, depends on the oscillating frequency ω for fixed oscillation amplitude. Interestingly, τ_n shows a clear-cut minimum at $\omega=\omega_c$, demonstrating that an oscillating field with an intermediate frequency can be the most favorable to the nucleation process. In ac-

*Author to whom correspondence should be addressed. E-mail: hzhlj@ustc.edu.cn

DOI:10.1088/1674-0068/25/04/419-422

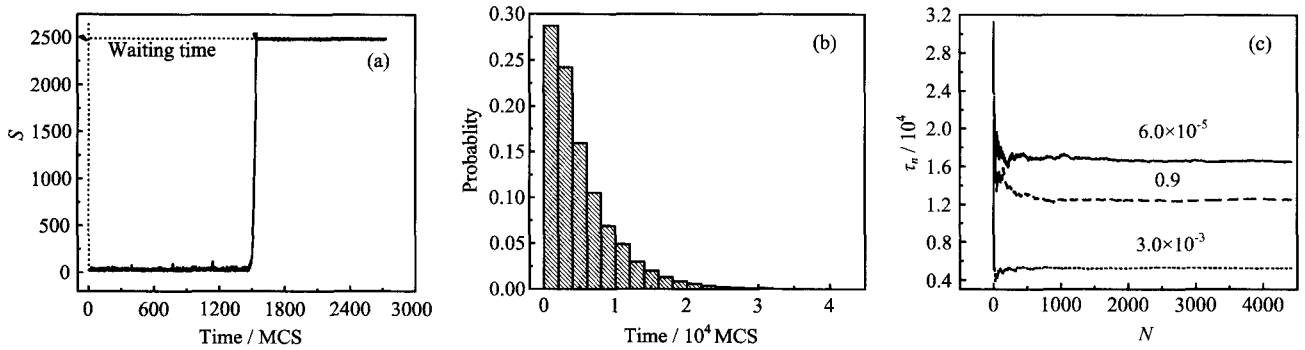

FIG. 1 (a) Time series S of up spins in a nucleation process. (b) Distribution of N_t at ω=3.0×10^{-3} for N=10×10^4 simulation runs. (c) Dependency of the average nucleation time τ_n on N for ω=6.0×10^{-5}, 3.0×10^{-3}, and 0.9.

cordance with this, we have investigated the mean size of the critical nuclei by analysis of the transition state ensemble. As expected, the average size of the critical nuclei is the smallest at ω_c. In addition, the effect of the initial phase ϕ of the external field on τ_n is also explored.

II. MODEL AND SIMULATION DETAILS

A ferromagnetically interacting nearest neighbor 2D Ising model in the presence of a time varying magnetic field can be represented by the Hamiltonian,

$$H = -J\sum_{\langle i,j\rangle} s_i s_j - h(t)\sum_i s_i \qquad (1)$$

here, J=1 is the coupling constant, s_i is the spin variable at site i which can be either +1 (up) or −1 (down), $\langle i,j\rangle$ represents nearest-neighbor pairs, and $\sum_i$ runs over all lattice sites. The external magnetic field $h(t)$ includes two components:

$$h(t) = h_0 + h_1\sin(\omega t + \phi) \qquad (2)$$

h_0>0 is a static field which is more favorable for up spins than down spins, and the second term is an oscillating field with amplitude h_1, frequency ω, and initial phase ϕ.

Initially, we set all the lattice spins down in h_0 always larger than h_1. By this setting, the initial state is metastable and the stable state is the one with most spins up. At a finite temperature, a phase transition will take place via a nucleation process from the initial state to the stable one. The configuration of the system is updated by Glauber standard dynamics: each attempt spin flip from s_i to $-s_i$ is accepted with probability

$$W(s_i \to -s_i) = \frac{\exp(-\beta\Delta E_i)}{1+\exp(-\beta\Delta E_i)} \qquad (3)$$

where ΔE_i is the energy change of the system if the spin flip is accepted and β=1/$k_B T$ with k_B the Boltzmann's constant and T the temperature. During the simulation, each lattice site is updated sequentially, and one such full scan over the lattice is defined as a Monte Carlo step (MCS). If not stated otherwise, all simulations are performed on a 50×50 lattice with h_0=0.17, h_1=0.04, and ϕ is randomly chosen from a uniform distribution from 0 to 2π. T=2/3T_c=1.54 where T_c is the critical temperature of the 2D Ising system out of the external field. Periodic boundary condition is imposed. Nucleation time for each frequency is obtained via averaging over 3000 independent simulation runs.

III. RESULTS

To describe the nucleation process, we chose the number of up spins S as the order parameter. The time series S for a typical nucleation process is shown in Fig.1(a), from which we can see that S fluctuates at low level in the early stage, which indicates the system is in the metastable state, followed by a sudden jump after a period of waiting time to the stable state with high value of S. Usually, the waiting time is randomly distributed as shown in Fig.1(b) for ω=3.0×10^{-3} for N=10×10^4 simulation runs. In Fig.1(c), the dependencies of τ_n on N are shown respectively for ω=6.0×10^{-5}, 3.0×10^{-3}, and 0.9. Obviously, τ_n converges after about 2000 runs. We thus define the average waiting time over N=3000 runs as the nucleation time τ_n (the nucleation rate R is simply 1/τ_n).

As already shown in Fig.1(c), τ_n for an intermediate ω, 3.0×10^{-3}, is smaller than that for a larger frequency ω and a smaller one. It seems that there exists an optimal frequency for the external field which is the most favorable for the nucleation process. To show this, we plot τ_n as a function of ω in Fig.2, where the dash-dot line denotes the nucleation time under the static field h_0. Indeed, τ_n exhibits a clear-cut minimum at some optimal frequency ω=ω_c. It is also shown that an external field with large frequency has no effect on the nucleation

DOI:10.1088/1674-0068/25/04/419-422

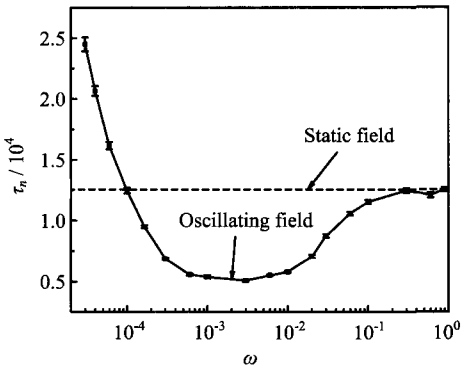

FIG. 2 Nucleation time τ_n as a function of the frequency ω. The dash-dot line represents the average waiting time in the static field h_0.

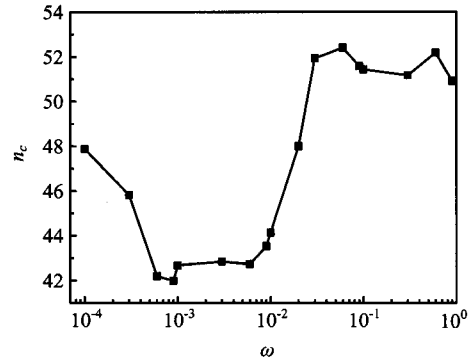

FIG. 3 The mean size of critical cluster n_c is plotted as function of frequency ω.

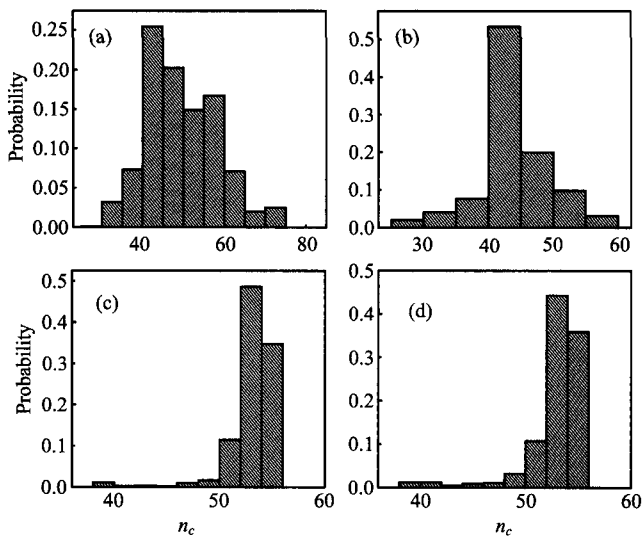

FIG. 4 Distribution of the size of critical nucleus at different frequency. (a) ω=1.0×10^{-4}. (b) ω=3.0×10^{-3}. (c) ω=0.9. (d) Static field h_0.

process. This is reasonable because in this case the period of the field is much smaller than τ_n and the system already oscillates many times in the metastable region before jumping to the stable state. In this case, the system can only experience an average field h_0. On the other hand, a slow-varying external field is not helpful for the nucleation process, the reason of which will be given below along with the discussion about the initial phase.

To further illustrate the existence of the optimal frequency, we tried to figure out the critical nucleus at different frequency by TSE sampling. TSE consists of a set of configurations located at the top of the free energy barrier along the nucleation pathway, wherein each configuration has the same probability to reach the final and the initial state. In simulations, we determine the transition state by computing the committor probability P_B which is the probability of reaching the final state before returning to the initial one for 4000 independent trials starting from this configuration. If a configuration with P_B=0.5±0.02, we take it as one belonging to the TSE. Analysis of the TSE containing 2000 configurations gives the information of the critical nucleus, the mean size n_c and distribution of which are obtained by the Hoshen-Kopelaman method [23].

Figure 3 shows the frequency ω dependence of n_c, which also exhibits an minimum for near ω_c. According to classic nucleation theory, a smaller critical nucleus size generally corresponds to a larger nucleation rate. Thus the tendency shown in Fig.3 is in agreement with Fig.2, which supports the existence of an optimal frequency. Accordingly, typical distributions of the nucleus size are shown in Fig.4 for ω=1.0×10^{-4}, 3.0×10^{-3}, 0.9 and h_0, respectively. For a low ω as shown in Fig.4(a), the distribution is relatively broad, indicating that a critical nucleus to some extent is not well-defined in this case. Near the optimal frequency, the distribution is more sharp around a relatively smaller value, see Fig.4(b). When ω is large, the distribution is biased to larger size, as depicted in Fig.4(c), which is very similar to the case for a static external field, see Fig.4(d).

To understand why τ_n in an oscillating field with very low frequency is much larger than that in a static field h_0, we have evaluated the effect of the initial phase ϕ on τ_n. Note that if ω tends to zero, the system is simply subjected to a field $h'=h_0+h_1 \sin\phi$. For the simulation results above, ϕ is randomly chosen from a uniform distribution from 0 to 2π. We now fix ϕ to see how it would influence τ_n, which is demonstrated in Fig.5. For very low frequencies, for instance ω=6.0×10^{-5}, 1.0×10^{-4}, and 3.0×10^{-4}, the curve of τ_n versus ϕ shows a sinusoidal-like shape, but being unsymmetric with respect to $\phi=\pi$. With decreasing frequency, the peak (right side) height of τ_n increases more rapidly than the valley (left side) depth decreases. Note that the ensemble average of the nucleation time for random initial phase equals the area below the curve. Therefore, the asymmetric distribution of τ_n with respect to ϕ is the

DOI:10.1088/1674-0068/25/04/419-422

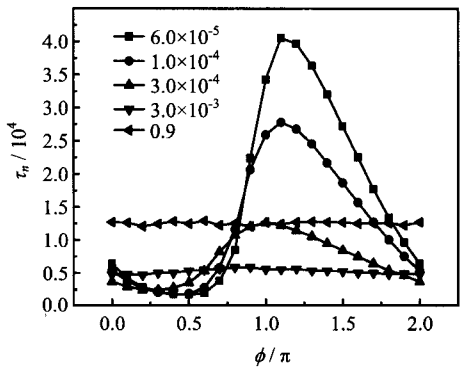

FIG. 5 The effect of initial phase ϕ in a definite frequency on the average nucleation time τ_n of varying initial phase. ω=6.0×10^{-5}, 1.0×10^{-4}, 3.0×10^{-4}, 3.0×10^{-3}, and 0.9. Each dot is also averaged by 3000 simulations.

very reason that leads to the increment of τ_n with decreasing ω shown in Fig.2. We also notice that for a relatively large ω, as also shown in Fig.5 for ω=3.0×10^{-3} and 0.9, τ_n is not sensitive to the fixed initial phase ϕ, but τ_n keeps an apparently smaller value for the former frequency which is closer to ω_c than the latter one.

IV. CONCLUSION

Nucleation of a 2D kinetic Ising model subject to a bias oscillating field has been studied. We find that there exists an optimal frequency of the external field which is the most favorable to the nucleation process. This is demonstrated by a clear-cut minimum of the nucleation time, as well as a smallest average size of the critical nucleus. We have also investigated the effect of initial phase of the external field on the nucleation time, which helps to illustrate why a slow varying field also slows down the nucleation process. Since the Ising model is widely used in many physical, chemical and biological systems, and periodic loading is often used to perform system control, our study may open new perspectives in the study of nonequilibrium nucleation process.

V. ACKNOWLEDGMENT

This work was supported by the National Natural Science Foundation of China (No.21125313, No.20933006, and No.91027012).

[1] D. Kashchiev, *Nucleation: Basic Theory with Applications*, Butterworths-Heinemann: Oxford, (2000).
[2] P. ten Wolde, M. Ruiz-Montero, and D. Frenkel, Phys. Rev. Lett. **75**, 2714 (1995).
[3] G. Johnson, A. I. Mel'cuk, H. Gould, W. Klein, and R. D. Mountain, Phys. Rev. E **57**, 5707 (1998).
[4] Z. P. Lu and C. Liu, Phys. Rev. Lett. **91**, 115505 (2003).
[5] A. R. Fersht, Curr. Opin. Struct. Biol. **7**, 3(1997).
[6] A. C. Pan and D. Chandler, J. Phys. Chem. B **108**, 19681 (2004).
[7] D. Wilms, A. Winkler, P. Virnau, and K. Binder, Comput. Phys. Commun. **182**, 1892 (2011).
[8] A. J. Page and R. P. Sear, Phys. Rev. Lett. **97**, 065701 (2006).
[9] V. A. Shneidman and K. M. B. K. A. Jackson, J. Chem. Phys. **111**, 006932 (1999).
[10] R. S. Graham and P. D. Olmsted, Phys. Rev. Lett. **103**, 115702 (2009).
[11] L. Chen, X. Wang, R. Straff, and K. Blizard, Polym. Eng. Sci. **42**, 1151 (2002).
[12] R. Blaak, S. Auer, D. Frenkel, and H. Löowen, Phys. Rev. Lett. **93**, 068303 (2004).
[13] G. Mazzanti, S. E. Guthrie, E. B. Sirota, A. G. Marangoni, and S. H. J. Idziak, Cryst. Growth Des. **3**, 721 (2003).
[14] R. J. Allen, C. Valeriani, S. Tanase-Nicola, P. R. ten Wolde, and D. Frenkel, J. Chem. Phys. **129**, 134704 (2008).
[15] T. Tome and M. J. de Oliveira, Phys. Rev. A **41**, 4251 (1990).
[16] M. Acharyya and B. K. Chakrabarti, Phys. Rev. B **52**, 6550 (1995).
[17] S. W. Sides, P. A. Rikvold, and M. A. Novotny, Phys. Rev. Lett. **81**, 834 (1998).
[18] G. Korniss, C. J. White, P. A. Rikvold, and M. A. Novotny, Phys. Rev. E **63**, 016120 (2000).
[19] D. T. Robb, P. A. Rikvold, A. Berger, and M. A. Novotny, Phys. Rev. E **76**, 021124 (2007).
[20] H. Fujisaka, H. Tutu, and P. A. Rikvold, Phys. Rev. E **63**, 036109 (2001).
[21] S. B. Dutta, Phys. Rev. E **71**, 066115 (1999).
[22] G. M. Buendia and P. A. Rikvold, Phys. Rev. E **78**, 051108 (2008).
[23] J. Hoshen and R. Kopelman, Phys. Rev. B **14**, 3438 (1976).

DOI:10.1088/1674-0068/25/04/419-422

Chinese Abstracts (本期中文摘要)
中国科学技术大学专辑

摘要： 用离子速度成像结合共振增强多光子电离技术研究了2-溴丁烷分子在264.77和264.86 nm(约265 nm)的光解离动力学．从获得的离子速度图像确定了光解产物Br和Br*碎片的速度分布和角度分布．其速度分布可以由一个窄的高斯分布拟合得到，它对应于沿着C−Br伸缩模式的直接解离．2-溴丁烷在约265 nm的光解离中$^1Q_1 \leftarrow {}^3Q_0$的非绝热跃迁在Br离子碎片的产生中起到非常重要的作用，确定Br($^2P_{3/2}$)的相对量子产额为0.621．通过约265和约234 nm处2-溴丁烷光解的比较发现，各向异性参数和相对量子产率随着波长增加而下降，$^3Q_0$和$^1Q_1$态势能面交叉几率随着波长增加而降低．
关键词： 2-溴丁烷，离子速度成像，光解离

摘要： 利用同步辐射光电离质谱结合理论计算，研究了异亮氨酸的真空紫外光诱导电离解离．在光子能量为13 eV的质谱中探测到了m/z=86、75、74、69、57、46、45、44、41、30、28、18的碎片离子．对于异亮氨酸的主要碎片离子为：$C_5H_{12}N^+$ (m/z=86)、$C_2H_5NO_4{}^+$ (m/z=75)、$C_5H_9{}^+$ (m/z=69)、$C_4H_9{}^+$(m/z=57)和CH_4N^+确良(m/z=30)．由光电离效率曲线得到出现势分别为：8.84±0.07、9.25±0.06、10.20±0.12、9.25±0.10、11.05±0.07 eV．结合量化理论计算(B3LYP/6-31++G(d,p))，详细给出了它们可能的生成路径．这些解离通道包括简单的键断裂反应和涉及中间体、过渡态的反应，实验值和理论计算的离子出现能或势垒一致．
关键词： 同步辐射，真空紫外，光电离质谱，异亮氨酸，解离通道

摘要： 使用1.54 μm的激光脉冲(脉宽约10 ns)诱导丹磺酰基标记的热敏性线性聚*N*-异丙基丙烯酰胺(PNIPAM)发生线团到小球的转变．当聚合物链中NIPAM单体与丹磺酰基基团的摩尔比由110增至300时，共价键合到聚合物主链上的丹磺酰基发色团对PNIPAM相转变行为的影响会随之减小．PNIPAM链塌缩经历成核过程(伴随着初始珍珠的形成，快弛豫时间τ_{fast}=0.1 ms)和珍珠的增长粗化阶段(慢弛豫时间τ_{slow}=0.5 ms)，这与之前使用水溶性的1-苯胺-8-萘磺酸铵盐作为荧光探针研究PNIPAM在水溶液中的折叠动力学得到的结果类似．τ_{fast}在很宽的分子量范围内都与分子量无关，而τ_{slow}则随链长增加而略有增大．
关键词： 荧光标记，激光光散射，相转变，刺激响应性聚合物

摘要： 使用基于密度泛函理论的CASTEP软件计算了BAM:Eu^{2+}($BaMgAl_{10}O_{17}:Eu^{2+}$)荧光粉在SiN掺杂前后的能带、态密度、吸收光谱和Mulliken布居．Eu^{2+}处于BR位置光吸收更强；SiN掺杂使处于BR位置的Eu^{2+}的数量上升，而处于mO位置的Eu^{2+}的数量下降，抵消了SiN掺杂降低Eu的态密度对光谱的影响．所以适量掺杂的SiN提高了BAM:Eu^{2+}荧光粉的吸收发射光谱强度．Si−N键和Eu−N键的Mulliken布居数分别高于Al−O键和Eu−O键，说明Si−N键和Eu−N键的共价性分别强于Al−O键和Eu−O键．发光中心Eu^{2+}局域结构共价性的增强降低了BAM:Eu^{2+}镜面层的活性，这是SiN掺杂提高BAM:Eu^{2+}荧光粉光学稳定性的主要原因．
关键词： 荧光粉，$BaMgAl_{10}O_{17}:Eu^{2+}$，SiN掺杂，第一性原理

摘要： 为了确定Si(111)-$\sqrt{7}\times\sqrt{3}$-In表面的结构以及理解其电子性质，构建了六角型和矩形型的六种模型，并进行了第一性原理计算．通过模拟这些模型的扫描隧道显微镜图像，计算了功函数，并和实验结果进行了比较．发现hex-H3′模型和rect-T1模型分别为实验中的六角型和矩形型结构．同时还讨论了In覆盖度在1.0单层附近时In/Si(111)表面结构的演化机制．认为4×1相和$\sqrt{7}\times\sqrt{3}$相具有两种不同的演化机制，和实验结果一致．
关键词： 表面重构，Si(111)-$\sqrt{7}\times\sqrt{3}$-In，密度泛函理论，扫描隧道显微镜图像

摘要： 同时考虑亮氨酸可能的水分子络合方式及亮氨酸分子的所有内轴转动，对亮氨酸与1~3个水分子的复合结构Leu-$(H_2O)_n$进行了系统寻找、分别用BHandHLYP/6-31+G*和BHandHLYP/6-311++G**方法对结构进行了优化和单点能计算．发现亮氨酸水合结构与孤立亮氨酸有着很好的对应关系，且亮氨酸的水合结构可以可靠地通过对亮氨酸的结构直接加水得到．对中性、双电性亮氨酸水合结构的红外计算光谱与溶液中亮氨酸实验光谱进行了比较与分析，发现双电性Leu-$(H_2O)_3$的红外光谱与实验符合得最好，表明溶质在气相中与适量的水分子络合便能较好地模拟溶质在溶液中的红外光谱．
关键词： 氨基酸，水合作用，第一性原理计算，势能面，红外光谱

摘要： 研究了二维的动力学伊辛模型在一个具有偏向的振荡外场中的成核过程，主要关注成核时间与外场振荡周期ω的关系．随着ω的变化，成核时间出现最小值，最小的成核时间对应的平均临界核的大小也是最小的，这表明存在一个最佳的振荡频率，相比较于一个确定的外场，它更有利于成核．同时还研究了外场的初始相位的影响．
关键词： 动力学伊辛模型，振荡外场，成核

摘要： 利用超高真空扫描隧道显微镜，在低温(80 K)下研究了同分异构体分子Dy@C_{82}在Au(111)表面的吸附与分子取向．在低覆盖度下，Dy@C_{82}分子优先吸附于台阶边缘形成分子团簇与分子链结构．这种吸附取决于分子-衬底的相互作用，并存在多种不同的分子取向．增大分子覆盖度后，Dy@C_{82}在金表面形成二维有序密排的单层膜结构．Dy@C_{82}分子在金表面的取向倾向于其C_2长轴与金表面近乎平行．具有三种取向的分子最具优势，而同种取向的分子组成许多局限于一个个小区域内的取向有序结构畴．随着覆盖度的增加，Dy@C_{82}分子在Au(111)表面趋向于短程有序取向排列，这是由分子-衬底作用与分子间的偶极-偶极作用共同决定的．
关键词： 金属包合富勒烯，扫面隧道显微镜，分子取向，单分子层

摘要： 利用固相法合成了钠掺杂的$LiFePO_4$，结构表征显示钠离子成功地掺入到了晶格中．SEM显示其粒径在1~3 μm．XRD显示钠掺杂样品晶胞变大．电池测试表明样品0.1 C放电150 mAh/g，5和7.5 C下分别放电109和107 mAh/g．1和5 C循环时，与初始放电容量相比，样品容量保持率分别为84%(1000次循环后)和86%(350次循环后)，表现了优异的结构稳定性和循环性能．研究表明钠离子掺杂可以有效地提高磷酸铁锂的电化学活性，尤其是循环性能．
关键词： 磷酸铁锂，钠离子掺杂，结构变化，循环性能，锂离子电池

摘要： 用分子动力学模拟方法研究了石墨炔膜对H_2/O_2、H_2/N_2、H_2/CO和H_2/CH_4混合气体的选择渗透性．在0.047~4.5 GPa的压强

DOI:10.1088/1674-0068/25/04/cabs